Identification and prognostic analysis of ferroptosis-related gene HSPA5 to predict the progression of lung squamous cell carcinoma

DI GUO, YONGHAI FENG, PEIJIE LIU, SHANSHAN YANG, WENFEI ZHAO and HONGYUN LI

Department of Respiratory and Critical Care Medicine, Fifth Affiliated Hospital of Zhengzhou University, Zhengzhou, Henan 450000, P.R. China

Received November 8, 2023; Accepted February 1, 2024

DOI: 10.3892/ol.2024.14320

Abstract. Ferroptosis, an iron-dependent form of regulated cell death driven by excessive lipid peroxidation, is implicated in the development and therapeutic responses of cancer. However, the role of ferroptosis-related gene profiles in lung squamous cell carcinoma (LSCC) remains largely unknown. The present study aimed to identify the prognostic roles of ferroptosis-related genes in LSCC. Sequencing data from the Cancer Genome Atlas were analyzed and ferroptosis-related gene expression between tumor and para-tumor tissue was identified. The prognostic role of these genes was also assessed using Kaplan-Meier analyses and univariate and multivariate Cox proportional hazards regression model analyses. Immunological correlation, tumor stemness, drug sensitivity and the transcriptional differences of heat shock protein (HSP)A5 in LSCC were also analyzed. Thereafter, the expression of HSPA5 in 100 patients with metastatic LSCC was evaluated using immunohistochemistry (IHC) and the clinical significance of these markers with different risk factors was assessed. Of the 22 ferroptosis-related genes, the expression of HSPA5, HSPB1, glutathione peroxidase 4, Fanconi anemia complementation group D2, CDGSH iron sulfur domain 1, farnesyl-diphosphate farnesyltransferase 1, nuclear factor erythroid 2 like 2, solute carrier (SLC)1A5, ribosomal protein L8, nuclear receptor coactivator 4, transferrin receptor and SLC7A11 was significantly increased in LSCC compared with adjacent tissues. However, only high expression of HSPA5 was able to predict progression-free survival (PFS) and disease-free survival in LSCC. Although HSPA5 was also significantly elevated in patients with lung adenocarcinoma, HSPA5 expression did not predict the prognosis of patients with lung adenocarcinoma. Of note, a higher expression of HSPA5 was related to higher responses to chemotherapy but not to immunotherapy. In addition, HSPA5 expression was positively correlated with 'ferroptosis', 'cellular responses to hypoxia', 'tumor proliferation signature', 'G2M checkpoint', 'MYC targets' and 'TGFB'. IHC analysis also demonstrated that a high expression of HSPA5 in patients with metastatic LSCC in the study cohort was associated with shorter PFS and overall survival. In conclusion, the present study demonstrated that the expression of the ferroptosis-related gene HSPA5 may be a negative prognostic marker for LSCC.

Correspondence to: Professor Hongyun Li, Department of Respiratory and Critical Care Medicine, Fifth Affiliated Hospital of Zhengzhou University, 3 Kangfu Front Street, Zhengzhou, Henan 450000, P.R. China
E-mail: lhyhxk@163.com

Abbreviations: NSCLC, non-small cell lung cancer; LSCC, lung squamous cell carcinoma; TCGA, The Cancer Genome Atlas; ICB, immune checkpoint blockade; RNA-Seq, RNA-sequencing; CDKN1A, cyclin-dependent kinase inhibitor 1A; HSP, heat shock protein; TTC35/EMC2, endoplasmic reticulum membrane protein complex subunit 2; SLC, solute carrier; NFE2L2, nuclear factor erythroid 2 like 2; MT1G, metallothionein-1G; GPX4, glutathione peroxidase 4; FANCD2, Fanconi anemia complementation group D2; CISD1, CDGSH iron sulfur domain 1; FDFT1, farnesyl-diphosphate farnesyltransferase 1; SAT1, spermidine/spermine N1-acetyltransferase 1; TFRC, transferrin receptor; RPL8, ribosomal protein L8; NCOA4, nuclear receptor coactivator 4; LPCAT3, lysophosphatidylcholine acyltransferase 3; GLS2, glutaminase 2; DPP4, dipeptidyl peptidase-4; CS, citrate synthase; ALOX15, arachidonate 15-lipoxygenase; ACSL4, acyl-CoA synthetase long-chain family member 4

Key words: NSCLC, LSCC, ferroptosis, HSPA5, prognosis, biomarkers

Introduction

As the leading cause of cancer-related death worldwide, lung cancer ranks first among malignant tumors in terms of both incidence and mortality rates (1). Non-small cell lung cancer (NSCLC) makes up 80-85% of all lung cancers and 50-70% of patients have distant metastasis at the time of diagnosis. The five-year survival rate of patients with NSCLC is <15-20% (2). A number of molecular targeted therapies and immunotherapies have markedly improved outcomes in NSCLC over the past two decades (3-8). However, the vast majority of advanced NSCLC cases become resistant to current treatments and eventually progress. Notably, among these, patients with lung squamous cell carcinoma (LSCC) is a special group that does not benefit from targeted therapy (9). Although immunotherapy has markedly improved the prognosis of patients with cancer, relatively low response rates and serious adverse events have hindered the clinical use of this promising treatment

in LSCC (9). Thus, identifying biomarkers is essential to screen populations with a dominance of treatment-responsive individuals for current therapies.

In the past decade, ferroptosis, an iron-dependent form of regulated cell death driven by excessive lipid peroxidation (10), has been implicated in the development and therapeutic responses of several types of cancer, including LSCC (11). The process of ferroptosis promotes and suppresses tumor development during tumorigenesis, which is triggered by the release of damage-associated molecules and the activation of immune responses triggered by ferroptotic damage within the tumor microenvironment (11). As ferroptosis influences the efficacy of chemotherapy, radiotherapy and immunotherapy, it is likely that these therapies may be improved by agents targeting ferroptosis signaling (10-15). It has been reported that numerous ferroptosis-related genes promote tumor growth and are potential targets for cancer treatment (11,14,15). Despite this, the prognostic impact of ferroptosis-related genes on cancers and the roles of ferroptosis-related genes in patients with LSCC remain unclear. Therefore, it is necessary to investigate the expression pattern and prognostic potential of ferroptosis-related genes in LSCC.

Using the Cancer Genome Atlas (TCGA) database, the present study assessed the expression levels of 22 ferroptosis-related genes in LSCC and para-cancerous tissues derived from previous studies. Furthermore, Kaplan-Meier survival analyses, univariate analyses and multivariate Cox analyses were performed and a nomogram based on the expression of heat shock protein (HSP)A5 was generated. In addition, the immune checkpoint blockade (ICB) responses, stemness features and half-maximal inhibitory concentration (IC_{50}) scores of chemotherapy drugs were evaluated. Thereafter, the prognostic significance of HSPA5 in metastatic LSCC in the study cohort was assessed. Accordingly, it may be hypothesized that HSPA5 expression can influence the outcome of LSCC and that higher expression of HSPA5 can be predicted by chemotherapy. In conclusion, the present study demonstrated that the expression of the ferroptosis-related gene HSPA5 is a negative prognostic marker for LSCC.

Materials and methods

Analysis of differential ferroptosis-related gene expression. RNA-sequencing (RNA-Seq) expression profiles for LSCC were downloaded from the TCGA database (https://www.cancer.gov/ccg/research/genome-sequencing/tcga) and the full TCGA-LSCC dataset (501 patients with LSCC, phs000178) was included in the present study. The ferroptosis-related genes presented in the present study were obtained from Liu *et al* (16). All of the analysis methods were implemented in R (version 4.0.3; R Foundation for Statistical Computing), as previously described (17-19).

Gene expression datasets and functional enrichment. The method used was similar to that of previous studies (17-20). The R software's 'limma' package was used to study differentially expressed mRNA. To identify mRNAs with differential expression, $P<0.05$ and $\log_2$ (fold change) >1 or $\log_2$ (fold change) <-1 were used as thresholds. An enrichment analysis of the Kyoto Encyclopedia of Genes and Genomes (KEGG) can be used to study gene function in conjunction with high-level genome functional information. KEGG pathways were enriched using the 'clusterProfiler' package (version 3.18.0) in R software to describe the carcinogenesis of mRNA. In addition, a box plot was created using R software with the 'ggplot2' package and a heat map with the 'pheatmap' package.

Kaplan-Meier survival analysis. In the present study, Kaplan-Meier survival analysis was divided into two parts: The first part was a Kaplan-Meier survival analysis (R software version 4.0.3) of the TCGA data. To generate Kaplan-Meier curves, log-rank tests were used to calculate P-values, hazard ratios (HRs) with 95% confidence intervals (CIs) and survival time between distinct groups. Disease-free survival (DFS) time was the period between the start of randomization and the time of the last follow-up visit or the time of death (from any cause). The progression-free survival (PFS) time was defined as the time between the start of randomization and the onset of (any aspect of) tumor progression, death (from any cause) or the last visit after the last randomization. The overall survival (OS) time was calculated from the time of randomization until death (from any cause) or the last follow-up visit. All of the analysis methods and R packages were implemented in R (version 4.0.3). $P<0.05$ was considered to indicate a statistically significant difference (21). The second part of the analysis was a Kaplan-Meier survival analysis of the cohort data of the present study. PFS and OS time for metastatic LSCC were compared for high and low expression of HSPA5 in the cohort and calculated using Kaplan-Meier analyses. The final follow-up was performed on May 1st, 2022.

Univariate analysis, multivariate Cox analysis and nomogram. As previously described, multivariate and univariate Cox regression analyses were performed to identify the suitable terms required for building a nomogram (22). A forest plot was used to show the P-value, HR and 95% CI of each variable with the 'forestplot' package in R software (version 4.0.3), and a nomogram was developed according to the results of the multivariate Cox proportional hazards analysis to predict the 1-, 3- and 5-year overall recurrence. The nomogram was used to provide a graphic representation of the factors used to calculate the risk of recurrence for an individual patient using the points associated with each risk factor through the 'rms' package in R software (version 4.0.3).

Cancer stemness analysis using the one-class logistic regression machine-learning algorithm. The mRNA stemness index was calculated using the machine-learning method of one-class logistic regression (OCLR) developed by Malta *et al* (23). Based on mRNA expression signatures, 11,774 genes were detected in the gene expression profile. Spearman's correlation coefficient was utilized to analyze the relationship between variables, followed by the transformation of the dryness index to a standardized range of [0,1] through a linear conversion involving subtraction of the minimum value and division by the maximum value. The aforementioned analysis methods and R packages were implemented in R software (version 4.0.3) as previously described (23).

Immune checkpoint analysis. SIGLEC15, TIGIT, CD274, HAVCR2, PDCD1, CTLA4, LAG3 and PDCD1LG2 were selected as immune checkpoint-relevant transcripts (24-29), and all the expression values of these eight genes were extracted. The aforementioned analyses and R packages were implemented in R software (version 4.0.3) using the 'ggplot2' and 'pheatmap' packages (version 4.0.3) (30-32).

ICB response analysis by tumor immune dysfunction and exclusion. First, the potential ICB response was predicted using a tumor immune dysfunction and exclusion (TIDE) algorithm as previously described (33). The TIDE algorithm uses a set of gene expression markers to assess two different mechanisms of tumor immune escape: Dysfunction of tumor-infiltrating cytotoxic T lymphocytes (CTLs) and exclusion of CTLs by immunosuppressive factors. High TIDE scores were associated with poor efficacy of ICB therapy and short survival time after administration of ICB therapy.

Signaling pathway analysis. The 'GSVA' package in R software (version 4.0.3) was used for the analysis, selecting the single-sample gene set enrichment analysis ('ssGSEA') method as a parameter. The correlation between genes and pathway scores was then analyzed using Spearman's correlation coefficient (34).

Chemotherapeutic sensitivity of LSCC. The chemotherapeutic response for each sample was predicted based on the largest publicly available pharmacogenomics database, the Genomics of Drug Sensitivity in Cancer (https://www.cancerrxgene.org/). The prediction process was implemented with the R package 'pRRophetic' (R Foundation for Statistical Computing, version 4.0.3). The IC_{50} of the samples was estimated by ridge regression. All parameters were set as the default values using the batch effect of combat and tissue type of all tissues, and the duplicate gene expression was summarized as the mean value.

Immunohistochemistry (IHC) and image analysis. Metastatic LSCC tissues and para-cancerous tissues (n=100) were obtained from the Fifth Affiliated Hospital of Zhengzhou University (Zhengzhou, China). A total of 100 patients were included in the study, which was performed from July 2015 to December 2018. All patients had undergone surgery and eventually developed lung metastases. These patients were treated according to the National Comprehensive Cancer Network guidelines for LSCC (35). Metastatic patients who have not undergone surgery are excluded. Formalin-fixed paraffin-embedding (FFPE) tissues were used in the present study and the detailed procedure was as described previously (36). In brief, the first step was to dewax and rehydrate formalin-fixed and paraffin-embedded sections of LSCC and para-cancerous tissues (5 μm thick). Antigen retrieval was performed by heating the slides in 10 mM Tris buffer with 1 mM EDTA (pH 9) in a streamer for 20 min. Samples were immersed in 3% H_2O_2 for 5 min to inhibit endogenous peroxidase activity. Subsequently, after Tris-buffered saline containing 0.1% Tween had been used for washing, endogenous biotin was inhibited by sequential incubation with 0.1% anti-biotin protein and 0.01% biotin (Dako; Agilent Technologies, Inc.) for 10 min at room temperature. Subsequently, 3% skimmed milk powder was applied for 30 min at room temperature to block unspecific binding. Thereafter, LSCC and para-cancerous tissue sections were incubated with HSPA5 monoclonal mouse anti-human antibodies (cat. no. ab21685; dilution, 1:1,000; Abcam) at 4˚C overnight. The sections were then serially rinsed and incubated with secondary antibody (cat. no. ab98799; dilution, 1:3,000; Abcam) at room temperature 1 h. Finally, color was developed by incubation with 3,3'-diaminobenzidine (DAB) substrate [ImmPACT DAB Peroxidase (HRP) substrate; cat. no. ab64238; Abcam], followed by counterstaining with hematoxylin for 5 min and mounting with Vecmount (cat. no. H-5000; Vector Laboratories). The IHC staining was evaluated independently by two experienced pathologists blinded to patient characteristics and results via microscopy (BX53; Olympus Corp.). Based on a combination of the % positive stained cells and the intensity of the staining, a semi-quantitative scoring system (H-score) was calculated, as previously described (32-34). The H-score was calculated as follows: [H-score=∑ % (0-100%) x intensity (1-3)]=(% weak-intensity cells x1) + (% moderate-intensity cells x2) + (% strong-intensity cells x3). The median H-score was selected as the cut-off value for high or low HSPA5 expression.

Statistical analysis. R software (version 4.0.3) was used for all statistical analyses of the TCGA data. The statistical details of all the experiments are reported in the Materials and methods section, including the statistical analyses performed and statistical significance. GraphPad Prism 9.0 (Dotmatics) and IBM SPSS Statistics 24.0 (IBM Corp.) were used to statistically analyze the cohort data. Quantification of the HSPA5 density was performed using an unpaired t-test, and PFS and OS were calculated using the Kaplan-Meier estimator. Univariate and multivariate Cox proportional hazards regression models were used to estimate the HRs, along with the associated CIs and P-values. The Student's unpaired t-test and the χ^2 test were used for inferential statistical analysis. For all data, $P<0.05$ was used to indicate a statistically significant difference.

Results

Expression distribution of ferroptosis-related genes in LSCC. An analysis of RNA-Seq data from the TCGA database was performed to determine the presence of ferroptosis-related genes in LSCC. Prior studies have identified 22 genes that have been reported to serve crucial roles in regulating ferroptosis (16). These ferroptosis regulator genes are CDKN1A, HSPA5, TTC35/EMC2, SLC7A11, NFE2L2, MT1G, HSPB1, GPX4, FANCD2, CISD1, FDFT1, SLC1A5, SAT1, TFRC, RPL8, NCOA4, LPCAT3, GLS2, DPP4, CS, ALOX15 and ACSL4. Following this, the expression patterns of ferroptosis-related genes in LSCC and adjacent tissues were compared. Of these 22 ferroptosis-related genes, the mRNA expression levels of HSPA5, HSPB1, GPX4, FANCD2, CISD1, FDFT1, NFE2L2, SLC1A5, RPL8, NCOA4, TFRC and SLC7A11 were significantly increased in LSCC compared with those in the adjacent tissues (Fig. 1). However, the expression levels of CDKN1A, EMC2, SAT1, LPCAT3, GLS2, DPP4, CS and ACSL4 were significantly decreased in LSCC compared with those in the adjacent healthy tissues (Fig. 1). However, there was no significant difference in the expression

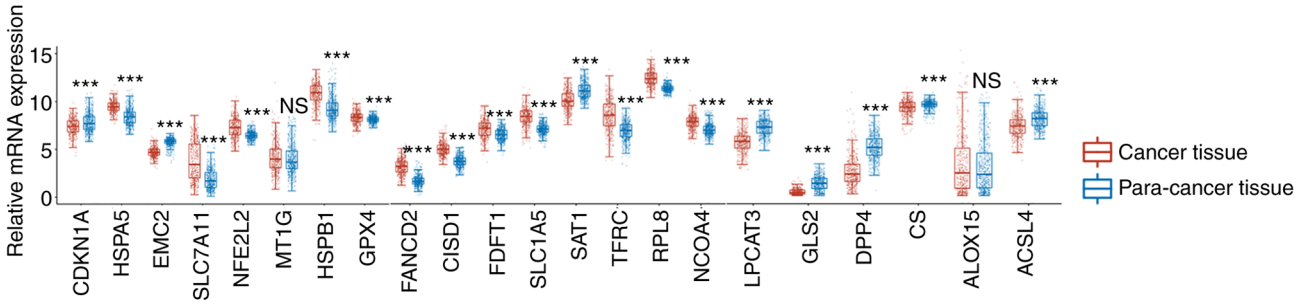

Figure 1. Relative mRNA expression of CDKN1A, HSPA5, EMC2, SLC7A11, NFE2L2, MT1G, HSPB1 and GPX4, FANCD2, CISD1, FDFT1, SLC1A5, SAT1, TFRC, RPL8, NCOA4, and LPCAT3, GLS2, DPP4, CS, ALOX15 and ACSL4 between lung squamous cell carcinoma and normal tissue. ***P<0.001. NS, not significant.

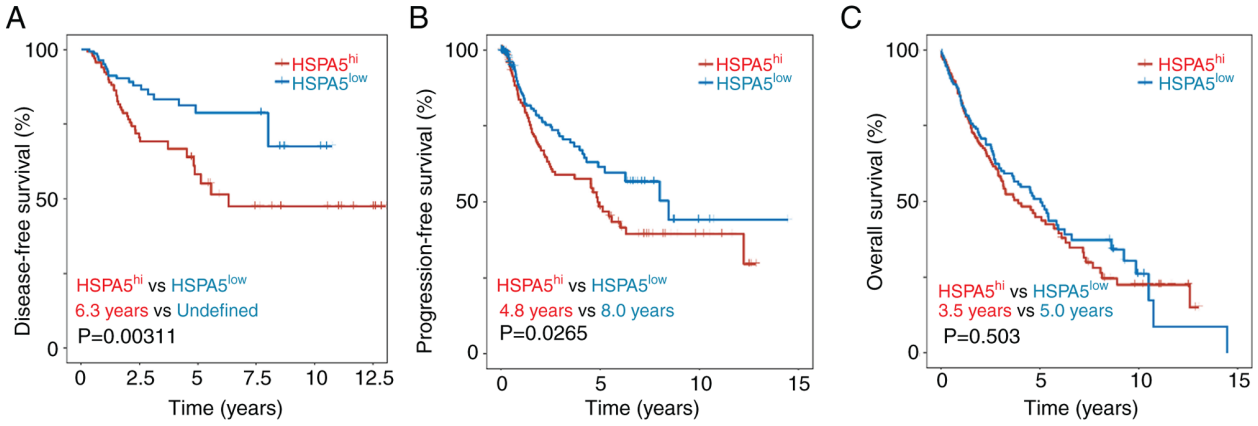

Figure 2. (A) Disease-free survival, (B) progression-free survival and (C) overall survival of patients with lung squamous cell carcinoma with high and low expression of HSPA5. HSPA5, heat shock protein A5.

levels of MT1G and ALOX15 in LSCC compared with those of the adjacent tissues (Fig. 1).

Different prognostic roles of ferroptosis-related genes in LSCC. Ferroptosis is involved in the metabolism of cells and the immune system, so it has been suggested that it and its regulators could be linked to cancer survival (37). In light of this, the prognostic value of increased ferroptosis-related gene expression was evaluated in LSCC. To determine whether ferroptosis-related gene expression is prognostic, the DFS, PFS and OS were evaluated. There were 12 genes related to ferroptosis with increased expression, and only the higher expression of HSPA5 was significantly associated with a shorter DFS (Fig. 2A) and PFS (Fig. 2B), but not OS (Fig. 2C). There was no significant difference in DFS, PFS or OS associated with high and low expression of the other 11 ferroptosis-related genes (Fig. S1). However, HSPA5 was significantly elevated in lung adenocarcinoma tissue compared with that of normal tissue (Fig. S2A). However, there was no significant difference in the DFS, PFS and OS between high and low expression of HSPA5 (Fig. S2B-D). Of the 22 ferroptosis-related genes, only HSPA5 predicted DFS, PFS and OS in patients with LSCC, suggesting that it may be a potential biomarker for predicting LSCC.

Both univariate and multivariate Cox analyses and the nomogram predict HSPA5 to be a poor prognostic factor for LSCC. A multivariate and univariate Cox analysis was performed to evaluate the independent prognostic value of HSPA5 in terms of DFS, PFS and OS of patients with LSCC. According to the univariate analysis, the group with high HSPA5 expression had a significantly worse DFS time (Fig. 3A) and the multivariate analysis demonstrated that high HSPA5 expression was independently associated with a significantly shorter DFS time (Fig. 3B). This result indicates that HSPA5 expression may serve as an independent prognostic factor for LSCC. To develop a clinically applicable method to predict a patient's survival probability, a nomogram was generated to construct a predictive model that considered clinicopathological covariates. With the multivariate and univariate analysis of DFS rates, a nomogram was created to predict the 1-, 3- and 5-year DFS rates in the discovery group, which demonstrates the similar results (Fig. 3C). The probability of the death of patients was also predicted using generalized linear regression. Among the predictors under evaluation was when $HSPA5^{hi}$ vs. $HSPA5^{low}$ met the P<0.05 risk assessment criterion. According to an ideal model, DFS rates in the entire cohort were well predicted at 1-, 3- and 5-year intervals (Fig. 3D). The independent prognostic significance of HSPA5 was then measured in terms of the PFS in patients with LSCC and the same results were obtained (Fig. 3E-H). By contrast, in terms of the OS of patients with LSCC, there were no significant differences between the HSPA5 high and low expression groups (Fig. S3). In summary, in both the univariate and multivariate Cox analysis, as well as the nomograms, HSPA5 was predicted to be an unfavorable prognostic factor.

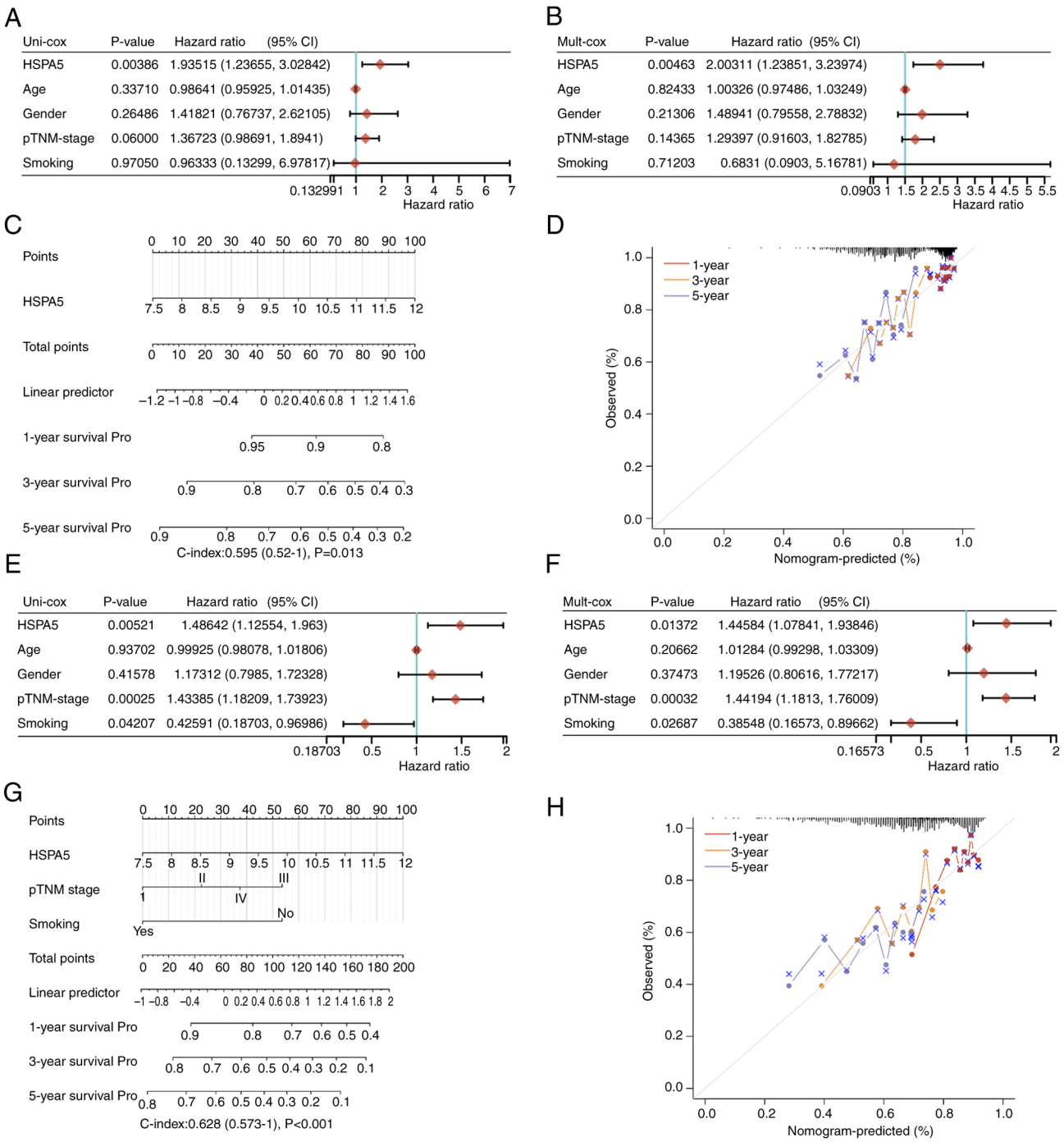

Figure 3. The (A) univariate and (B) multivariate Cox regression revealing the HRs and P-values and certain parameters of the HSPA5, p-TNM stage, age, gender and smoking of DFS. (C) Nomogram predicting the 1-, 3- and 5-year DFS of patients with LSCC. (D) Calibration curve for the DFS nomogram in the discovery group. The dashed diagonal line represents an ideal nomogram, whereas the red, orange and blue-gray lines represent the 1-, 3- and 5-year nomograms, respectively. The (E) univariate and (F) multivariate Cox regression revealing the HRs and P-values and certain parameters of the HSPA5, p-TNM stage, age, gender and smoking of PFS. (G) Nomogram predicting the 1-, 3- and 5-year PFS of patients with LSCC. (H) Calibration curve for the PFS nomogram in the discovery group. The dashed diagonal line represents an ideal nomogram, whereas the red, orange and blue-gray lines represent the 1-, 3- and 5-year nomograms, respectively. HR, hazard ratio; DFS, disease-free survival; HSPA5, heat shock protein A5; p-TNM, pathological Tumor-Node-Metastasis; LSCC, lung squamous cell carcinoma; PFS, progression-free survival.

High HSPA5 expression is associated with low responses to ICB via increased stemness of LSCC. Immune checkpoint inhibitors have become a common type of immunotherapy for patients with lung cancer in recent years (38,39). In the present study, TIDE scores were used to evaluate the ICB responses of patients with LSCC with high ($HSPA5^{hi}$) and low ($HSPA5^{low}$) expression of HSPA5. $HSPA5^{hi}$ patients had significantly higher TIDE scores than $HSPA5^{low}$ patients, indicating lower responses to ICB (Fig. 4A). Due to the strong association between immune checkpoint molecules and ICB responses, the expression of immune checkpoint molecules in patients with LSCC with $HSPA5^{hi}$ and $HSPA5^{low}$ was then assessed. PDCD1LG1, CTLA4 and PDCD1LG2 were all significantly upregulated, but not TIM3, LAG3, PDCD1, TIGIT and

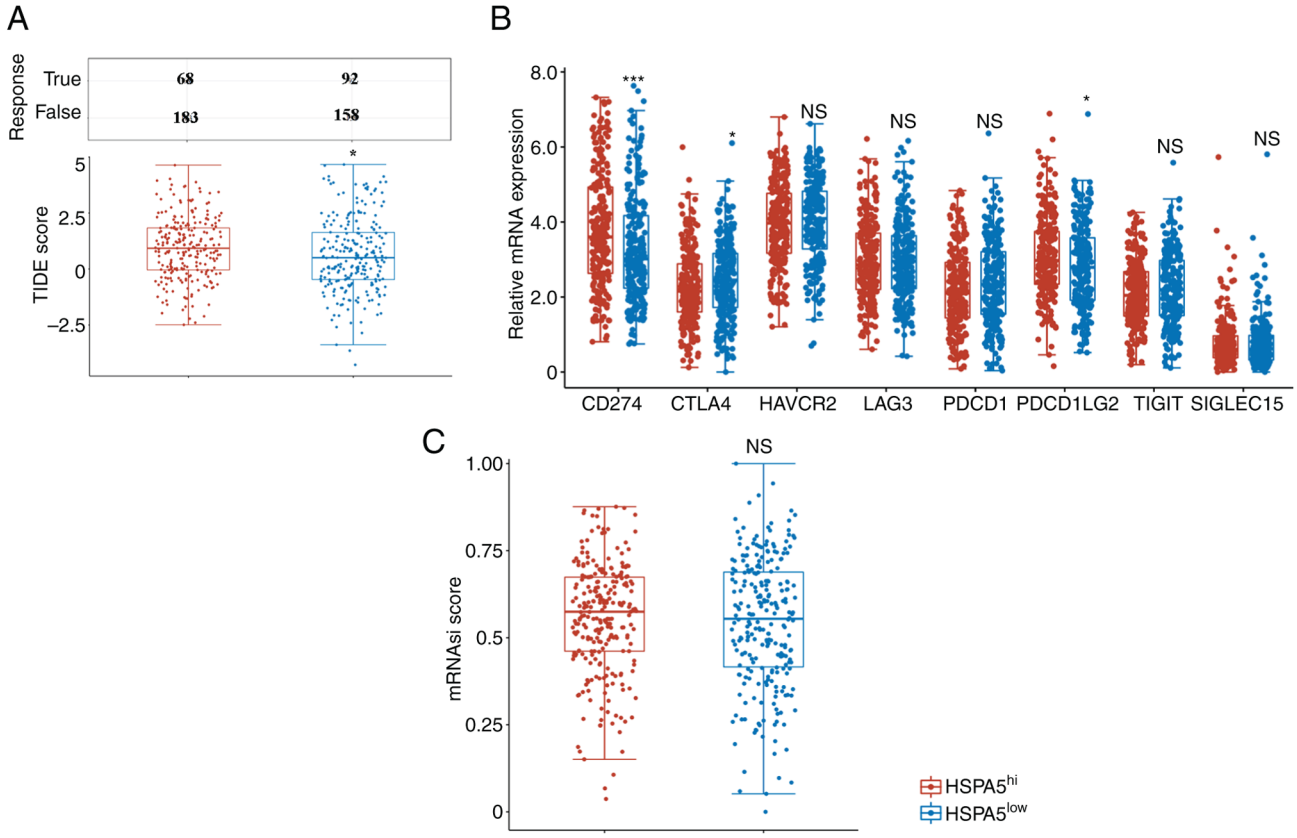

Figure 4. (A) Distribution of TIDE scores in the HSPA5^{hi} and HSPA5^{low} groups within the prediction results. (B) Expression of immune checkpoint molecules in the HSPA5^{hi} and HSPA5^{low} groups. (C) Distribution of mRNAsi scores in the HSPA5^{hi} and HSPA5^{low} groups within the prediction results. *P<0.05, ***P<0.001. NS, not significant; TIDE, tumor immune dysfunction and exclusion; HSPA5, heat shock protein A5; HSPA5^{hi}, high expression of HSPA5; mRNAsi, stemness index; PD-L1, programmed cell death-ligand 1; CTLA4, cytotoxic T lymphocyte-associated antigen 4; HAVCR2, hepatitis A virus cellular receptor 2; LAG3, lymphocyte activating 3; PDCD1, programmed cell death 1; PDCD1LG2, PDCD1 ligand 2; TIGIT, T-cell immunoreceptor with Ig and ITIM domains; SIGLEC15, sialic acid binding Ig like lectin 15.

SIGLEC15, in the HSPA5^{hi} group (Fig. 4B). Previous studies have indicated that cancer progresses through the gradual loss of a differentiated phenotype and the acquisition of stem-cell-like characteristics (23). Consequently, numerous treatment approaches, including immunotherapy, do not kill cancer stem cells effectively (40,41). Therefore, the stemness features of patients with LSCC with HSPA5^{hi} and HSPA5^{low} were tested using an OCLR machine-learning algorithm, as previously described (23). Patients with LSCC with HSPA5^{hi} were demonstrated to have similar OCLR scores to those with HSPA5^{low} (Fig. 4C). In summary, these data indicate that patients with LSCC with HSPA5^{hi} are not sensitive to ICB.

Differentially expressed genes and KEGG pathway analysis based on high and low expression of HSPA5. As HSPA5 can be used as a prognostic biomarker for lung adenocarcinomas, high and low expression levels of HSPA5 of patients with lung carcinomas were compared. The volcano plot in Fig. 5A depicts the 237 upregulated and the 27 downregulated genes in the HSPA5^{hi} vs. HSPA5^{low} groups (Table SI) and Fig. 5B presents a heat map of the differentially expressed genes. The KEGG signaling pathways enriched with differentially expressed genes were analyzed to predict their primary biological actions. Fig. 5C shows the KEGG pathways enriched by the upregulated genes in the HSPA5^{hi} vs. HSPA5^{low} group, including 'glutathione metabolism', 'focal adhesion', 'extracellular matrix (ECM)-receptor interaction' and numerous cancer pathways. Fig. 5D presents the KEGG pathways enriched by the downregulated genes in the HSPA5^{hi} vs. HSPA5^{low} group, including 'tyrosine metabolism', 'fatty acid degradation' and 'ATP-binding cassette transporters'. Correlations between the expression of HSPA5 with enriched signaling pathways with the use of ssGSEA analyses were also assessed, as previously described (42). Notably, positive correlations between HSPA5 expression and 'ferroptosis', 'cellular responses to hypoxia', 'tumor proliferation signature', 'G2M checkpoint', 'MYC targets' and 'TGFB' were demonstrated (Fig. 6).

High HSPA5 expression predicts distinct responses to chemotherapy for patients with LSCC. Cisplatin, gemcitabine, docetaxel, paclitaxel and vinorelbine are the five most commonly used chemotherapy agents in the treatment of LSCC (43,44). The present study therefore assessed whether high or low HSPA5 expression was associated with sensitivity to treatment with the five different chemotherapeutic agents commonly used for LSCC by IC_{50} analysis (Fig. 7). The IC_{50} scores for cisplatin, gemcitabine, docetaxel, paclitaxel and vinorelbine were tested according to previous reports (45). Patients with LSCC in the HSPA5^{hi} group exhibited significantly lower gemcitabine, docetaxel, paclitaxel and vinorelbine IC_{50} scores than those of the HSPA5^{low} group (Fig. 7B-E); however, the IC_{50} scores were similar between

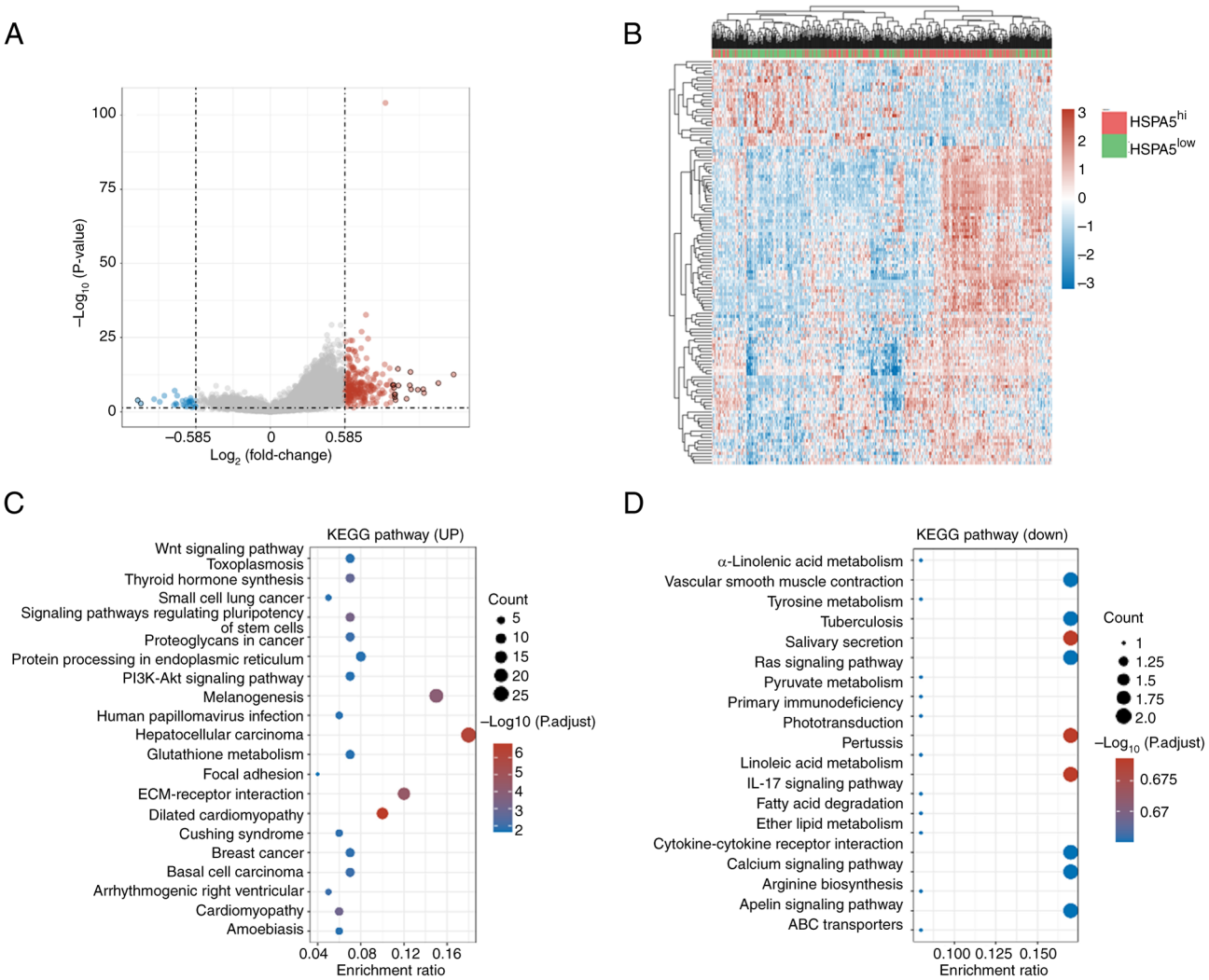

Figure 5. (A) Volcano plots of differentially expressed genes constructed using fold-change values and adjusted P-values in the HSPA5^{hi} and HSPA5^{low} groups. Red points represent the upregulated mRNAs, whereas blue points indicate the downregulated mRNAs, with statistical significance. (B) Heatmap of differentially expressed genes in the HSPA5^{hi} and HSPA5^{low} groups. KEGG signaling pathways enriched by the (C) upregulated and (D) downregulated genes in the HSPA5^{hi} lung squamous cell carcinoma group. HSPA5, heat shock protein A5; HSPA5^{hi}, high expression of HSPA5; KEGG, Kyoto Encyclopedia of Genes and Genomes; ECM, extracellular matrix; ABC, ATP-binding cassette.

groups for cisplatin (Fig. 7A). According to these results, patients with LSCC with HSPA5^{hi} may be more sensitive to chemotherapy.

High HSPA5 expression predicts poor prognosis in LSCC in the study cohort. A total of 100 metastatic LSCC tissues and para-cancerous tissues were obtained from the Fifth Affiliated Hospital of Zhengzhou University (Zhengzhou, China) to confirm the expression pattern of HSPA5. A total of 100 patients, of whom 47 (47%) were male and 53 (53%) were female, with a median age of 63 years, were included in the study, which was conducted from July 2015 to December 2018. All patients had undergone surgery and eventually developed lung metastases. These patients were treated according to the National Comprehensive Cancer Network guidelines for LSCC (35). Table I lists the detailed clinicopathological characteristics of the patients. To detect HSPA5 expression in each patient, IHC was performed with an anti-HSPA5 antibody. In Fig. 8A, representative IHC images of HSPA5 in cancerous and paraneoplastic tissues are provided. H-scores were used to perform a semiquantitative analysis of HSPA5 expression, as previously described (42). According to the quantitative analysis, the H-scores of HSPA5 in cancerous tissues were significantly higher than those in paraneoplastic tissues (Fig. 8B). Furthermore, it was demonstrated that the HSPA5 expression levels were different in every LSCC sample (Fig. 8B). The prognostic value of HSPA5 expression was then evaluated. The median H-score was used as a cut-off value for determining high and low expression of HSPA5. On the basis of the cutoff value for LSCC, the LSCC group of patients was divided into high-expression (HSPA5^{hi}) and low-expression (HSPA5^{low}) subgroups. The PFS and OS of the patients with HSPA5^{hi} and HSPA5^{low} metastatic LSCC was then evaluated. In line with the results for the TCGA database cohort, higher expression of HSPA5 in metastatic LSCC was significantly associated with shorter PFS (Fig. 8C) and OS (Fig. 8D). Furthermore, univariate analysis revealed that an advanced tumor-node-metastasis (TNM) stage (46) was a risk factor for PFS and OS (Table II). These risk factors from the univariate

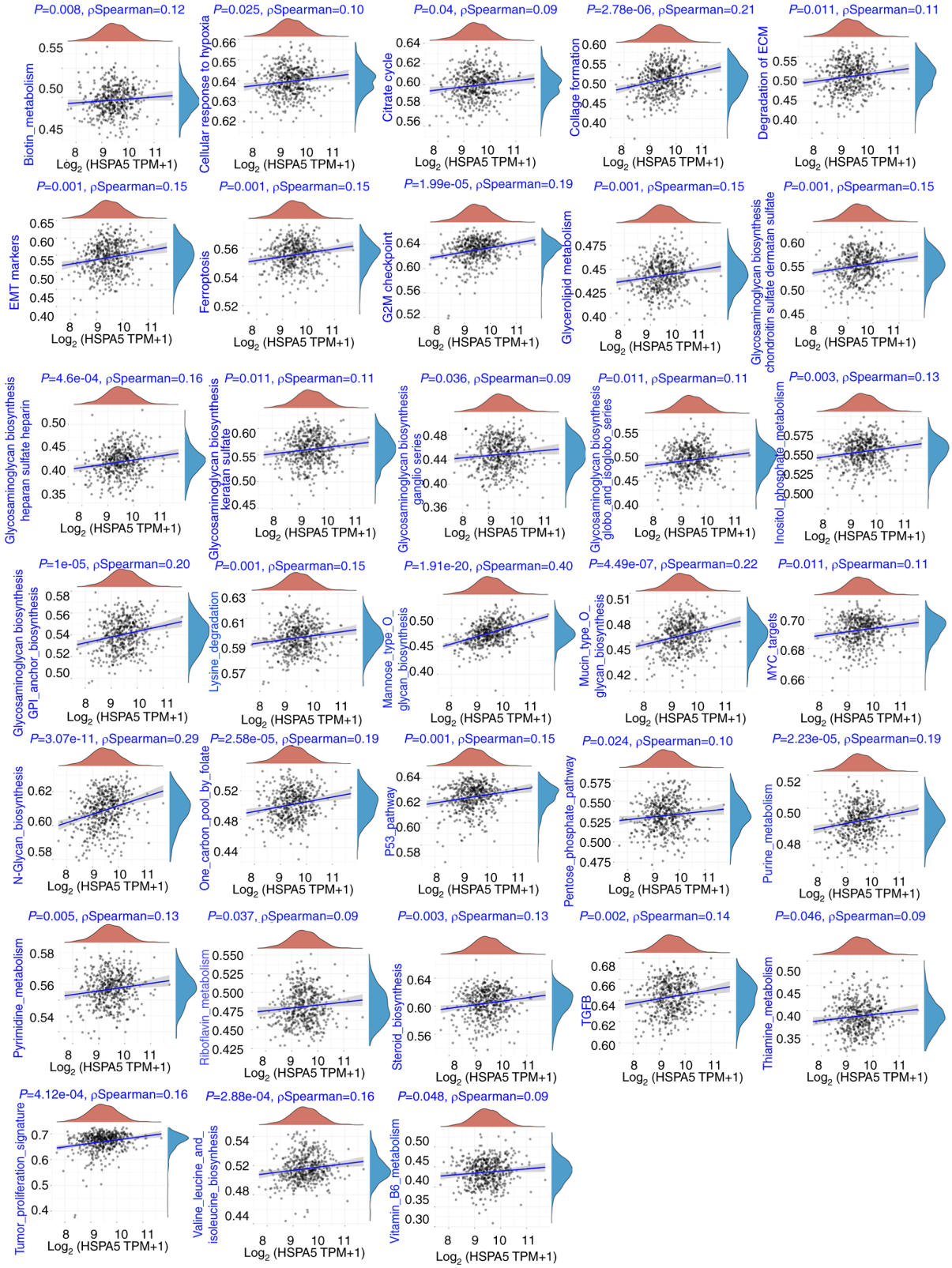

Figure 6. Correlations between HSPA5 expression and the pathway score assessed using Spearman's correlation coefficient. The abscissa represents the distribution of HSPA5 expression, whereas the ordinate represents the distribution of the pathway score. HSPA5, heat shock protein A5; TPM, transcripts per million.

analysis were adopted as covariates in a multivariate Cox proportional hazards model, and an advanced TNM stage and HSPA5 were determined to be independent prognostic indicators for PFS and OS (Table III).

Discussion

NSCLC is the most common malignancy in the world, with the highest incidence and mortality rates (47). In recent years,

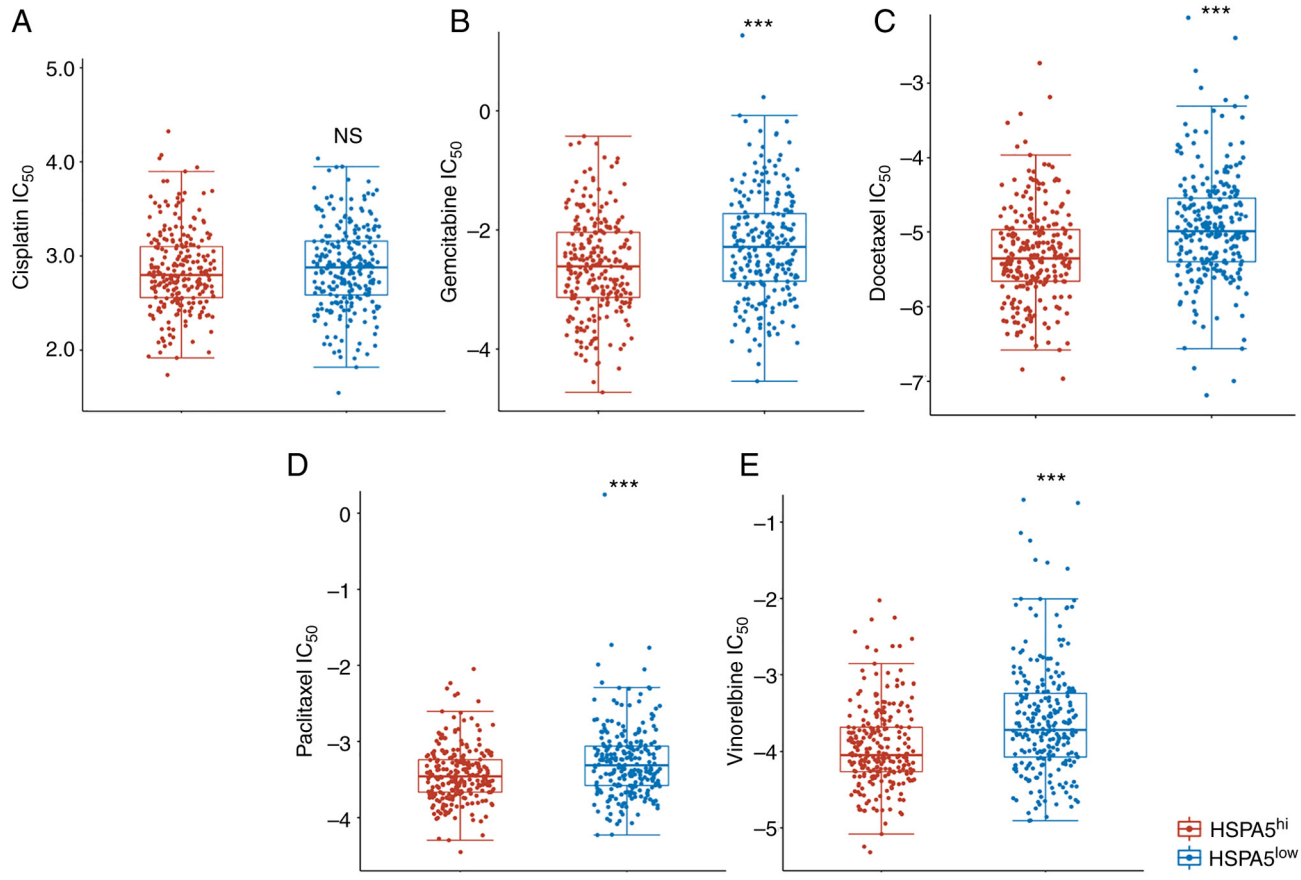

Figure 7. Difference in the IC_{50} values of (A) cisplatin, (B) gemcitabine, (C) docetaxel, (D) paclitaxel and (E) vinorelbine in the $HSPA5^{hi}$ and $HSPA5^{low}$ groups. ***P<0.001. NS, not significant; HSPA5, heat shock protein A5; $HSPA5^{hi}$, high expression of HSPA5; IC_{50}, half-maximal inhibitory concentration.

advances in immunotherapy and targeted treatments have significantly improved patient outcomes in lung adenocarcinoma. Despite this, the 5-year survival rate of these patients remains <20% (1,3-8). However, patients with LSCC cannot benefit from targeted therapy (9), and low response rates and serious adverse events have hindered the clinical use of immunotherapy in LSCC. Several parameters have been evaluated for clinical decisions and prognostication of lung cancer (48-50). However, emerging clinical evidence has shown that patients at the same TNM stage undergoing the same treatment have different prognoses, which indicates that prognosis assessments based on the TNM stage alone may not be adequate in the context of LSCC (51,52).

Ferroptosis has been associated with cancer development and represents a promising treatment strategy for cancer (11,14,15,37). In this regard, modulating the progress of ferroptosis may affect the proliferation, colony formation and cell death of lung cancer cells and improve the therapeutic efficacy of xenografts for lung cancer (53). Nevertheless, ferroptosis-related gene profiling remains to be clarified as a prognostic factor in the context of LSCC. In the present study, the TCGA database was used to assess the variations in expression profiling of ferroptosis-related genes in LSCC. Through these analyses, the signature of 22 ferroptosis-related genes was identified, and it was demonstrated that, of these genes, the expression of HSPA5, HSPB1, GPX4, FANCD2, CISD1, FDFT1, NFE2L2, SLC1A5, RPL8, NCOA4, TFRC and SLC7A11 was significantly increased in LSCC. Thereafter, the association between ferroptosis-related genes and the prognosis of patients with LSCC was evaluated. The survival analysis found that, of the 11 ferroptosis-related genes with increased expression, only HSPA5 was highly related to the DFS and PFS of patients with LSCC. The results of the present study on patients with metastatic LSCC revealed that higher levels of HSPA5 expression predicted poor prognosis and shorter PFS and OS. Furthermore, the results indicated that increased HSPA5 expression may also assist with the prediction of metastatic LSCC.

HSPA5 is a member of the HSP 70 superfamily, which serves as an important regulator in numerous diseases (54). HSPA5 is also related to the progression of certain cancers, including head and neck cancer, endometrial cancer, liver cancer, glioblastoma, breast cancer and osteosarcoma. In addition, it has been reported that HSPA5 is closely associated with the progression and poor prognosis of NSCLC, and serves an important role in the treatment of NSCLC (55). Lung adenocarcinoma and LSCC are important types of NSCLC; however, they are two different tumor types with relatively specific aspects in terms of diagnosis, treatment and prognosis. However, the expression of HSPA5 markedly increases in both lung adenocarcinoma and LSCC. Using TCGA datasets, the present study demonstrated that higher expression of HSPA5 was associated with shorter DFS and PFS of patients with LSCC but not lung adenocarcinoma. In addition, multivariate and univariate Cox regression analyses were performed to demonstrate that the expression of HSPA5 is a prognostic marker for LSCC. In conclusion,

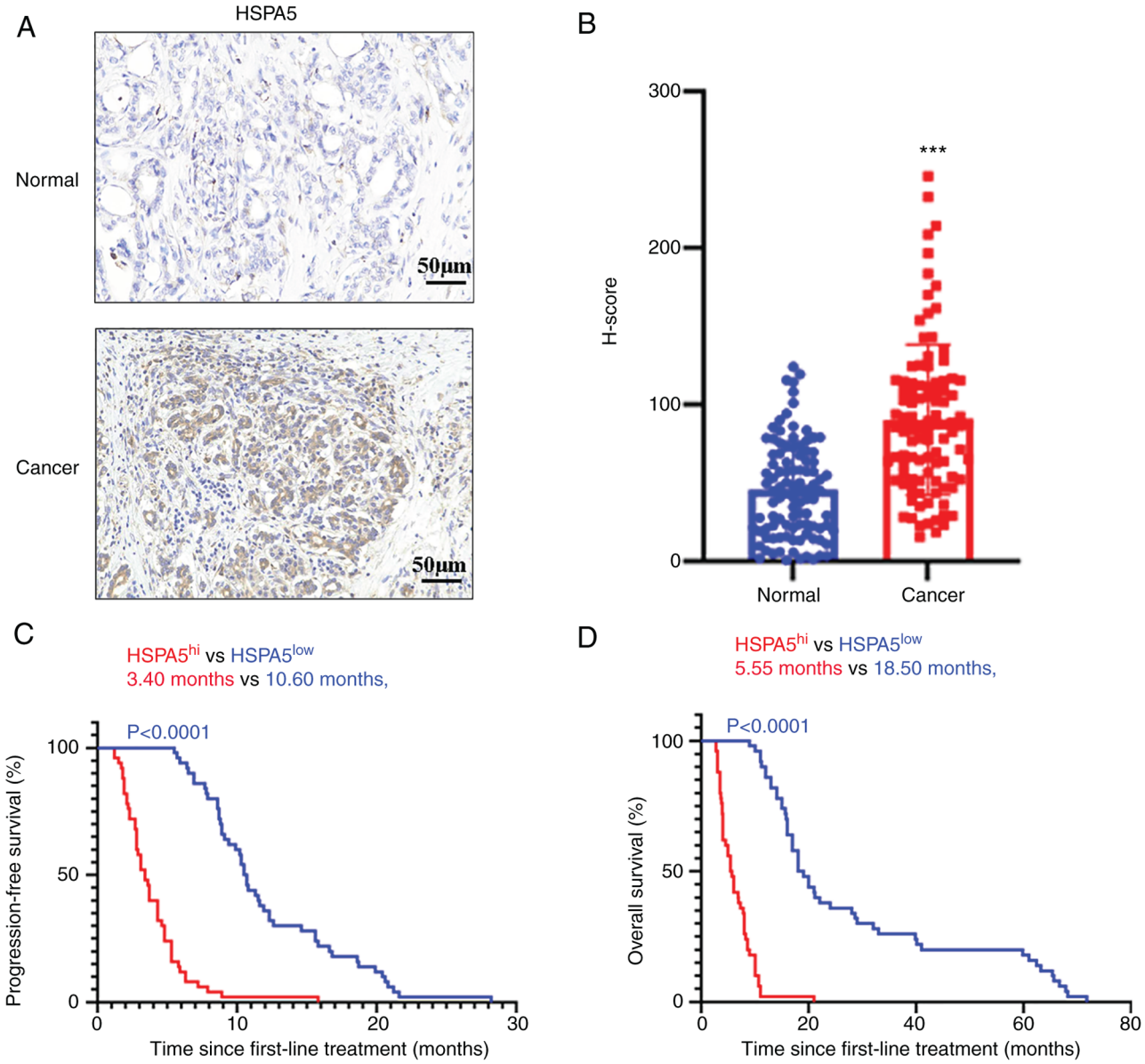

Figure 8. (A) Representative immunohistochemistry images of HSPA5 in LSCC and normal tissues (scale bars, 50 μm). (B) Quantitative analysis of the H-score indicating the expression of HSPA5 in LSCC and normal tissues. (C) Progression-free survival and (D) overall survival of LSCC in the high and low HSPA5 expression groups. ***P<0.001. HSPA5, heat shock protein A5; HSPA5^{hi}, high expression of HSPA5; LSCC, lung squamous cell carcinoma.

the present study further clarified that HSPA5 may be a useful prognostic predictor for LSCC.

In general, immune cells regulate tumor ferroptosis during cancer immunotherapy (56). Ferroptosis also regulates immune activity within tumor microenvironments (57). However, ferroptosis is largely unknown as a predictor of ICB responses in patients with LSCC. The present study demonstrated that individuals with higher expression levels of HSPA5 had worse TIDE scores, which indicates lower ICB responses. Therefore, HSPA5 expression may offer a novel means of predicting ICB responses. Nevertheless, further studies are required to identify the role of HSPA5 in immunotherapy for LSCC.

As a consequence of the aforementioned findings, differentially expressed genes and KEGG pathways associated with high and low levels of HSPA5 expression were assessed in patients with LSCC. Notably, it was demonstrated that high HSPA5 expression was associated with glutathione metabolism, focal adhesion, ECM-receptor interaction and numerous cancer pathways, which may accelerate tumor progression. In addition, ssGSEA signaling pathway analysis was performed for HSPA5 expression in LSCC, which demonstrated that the expression of HSPA5 was positively associated with 'ferroptosis', 'cellular responses to hypoxia', 'tumor proliferation signature', 'G2M checkpoint', 'MYC targets' and 'TGFB'. These findings revealed that high expression of HSPA5 may promote tumor progression through multiple mechanisms.

As there are no proven targeted drugs for LSCC, cisplatin-containing chemotherapy regimens (in combination with gemcitabine, docetaxel, paclitaxel and vinorelbine) are the first-line treatment option for patients with metastatic LSCC (58). However, not all patients are sensitive to chemotherapy. The IC_{50} is a method for assessing the effectiveness of a drug. The present study found that patients with LSCC with a higher expression of HSPA5 had lower IC_{50} scores for

Table I. Characteristics of patients with lung squamous cell carcinoma included from the cohort of the present study.

Characteristic	Patients (n=100)
Sex	
Male	43 (43)
Female	57 (57)
Age, years	62.8 (40-70)
Smoking history	
Yes	45 (45)
No	55 (55)
ECOG PS	
0	84 (84)
1	16 (16)
Size of primary tumor, cm	
≥5	39 (39)
<5	61 (61)
Histopathological grading	
High	8 (8)
Intermediate	43 (43)
Low	49 (49)
TNM stage	
IVA	44 (44)
IVB	56 (56)

Values are expressed as n (%) or median (range). ECOG PS, Eastern Cooperative Oncology Group Performance Status; TNM, tumor-node-metastasis.

Table II. Univariate analysis.

A, Progression-free survival

Parameter	Hazard ratio	95% CI	P-value
TNM stage (IVA vs. IVB)	2.56	(1.53, 3.16)	0.005
HSPA5 (high vs. low)	3.48	(1.87, 4.55)	0.003

B, Overall survival

Parameter	Hazard ratio	95% CI	P-value
TNM stage (IVA vs. IVB)	1.89	(0.99-2.17)	0.006
HSPA5 (high vs. low)	2.68	(1.38-3.24)	0.005

TNM, tumor-node-metastasis; HSPA5, heat shock protein A5.

Table III. Multivariate analysis.

A, Progression-free survival

Parameter	Hazard ratio	95% CI	P-value
TNM stage (IVA vs. IVB)	2.77	(1.88, 3.46)	0.004
HSPA5 (high vs. low)	2.33	(1.21, 3.65)	0.005

B, Overall survival

Parameter	Hazard ratio	95% CI	P-value
TNM stage (IVA vs. IVB)	1.58	(0.84-1.96)	0.008
HSPA5 (high vs. low)	1.67	(0.79-2.17)	0.009

TNM, tumor-node-metastasis; HSPA5, heat shock protein A5.

gemcitabine, docetaxel, paclitaxel and vinorelbine. However, there were no significant differences in IC_{50} values for cisplatin for high and low expression of HSPA5. In combination, the results highlight that the expression of HSPA5 may be regarded as a sufficient biomarker for predicting clinical responses to gemcitabine, docetaxel, paclitaxel and vinorelbine in the context of LSCC. Although a high HSPA5 expression predicts that LSCC patients should be more sensitive to chemotherapy, patients with high HSPA5 expression have worse DFS and PFS, which suggests rapid recurrence/metastasis after treatment in this group of patients. As mentioned above, the expression of HSPA5 was positively correlated with the tumor proliferation signature. Therefore, it is unsurprising that the worse prognosis of patients with high HSPA5 expression who are sensitive to chemotherapy may be related to the high proliferative characteristics of this group of patients. Therefore, it is important to assess the IC_{50} scores of other drugs for LSCC in the future, and it is also important to explore the potential mechanism of HSPA5 expression and chemosensitivity.

The present study has several limitations. It remains unclear how ferroptosis may contribute to the outcome of LSCC and how HSPA5 may initiate ferroptosis in LSCC. In addition, the expression of HSPA5 was only confirmed in metastatic LSCC. More studies should be conducted to confirm the present results and samples from patients with early- or late-stage LSCC should also be included. However, the expression of HSPA5 may still be an effective predictor of LSCC prognosis. Therefore, further studies are required to verify the role and function of HSPA5 in LSCC.

Acknowledgements

Not applicable.

Funding

No funding was received.

Availability of data and materials

The data generated in the present study may be requested from the corresponding author.

Authors' contributions

DG designed the study, performed the research, analyzed the data and drafted the manuscript. YF, PL, SY and WZ collected samples and performed analyses. HL designed the study and edited the manuscript. All authors have read and approved the final manuscript. DG and HL confirm the authenticity of all the raw data.

Ethics approval and consent to participate

Institutional review board approval and data sharing agreements were obtained from Zhengzhou University (Zhengzhou, China; approval no. ZZU-LAC-20220415). All procedures performed were in accordance with the ethical standards of the Institutional and/or National Research Committee and with the 1964 Helsinki Declaration and its later amendments or comparable ethical standards. Written informed consent was obtained from all patients for the retention of diagnostic samples for future experimental use at the time of collection.

Patient consent for publication

Not applicable.

Competing interests

The authors declare that they have no competing interests.

References

1. Wang M, Herbst RS and Boshoff C: Toward personalized treatment approaches for non-small-cell lung cancer. Nat Med 27: 1345-1356, 2021.
2. Global Burden of Disease Cancer Collaboration; Fitzmaurice C, Allen C, Barber RM, Barregard L, Bhutta ZA, Brenner H, Dicker DJ, Chimed-Orchir O, Dandona R, *et al*: Global, regional, and national cancer incidence, mortality, years of life lost, years lived with disability, and disability-adjusted life-years for 32 cancer groups, 1990 to 2015: A systematic analysis for the global burden of disease study. JAMA Oncol 3: 524-548, 2017.
3. Chaft JE, Rimner A, Weder W, Azzoli CG, Kris MG and Cascone T: Evolution of systemic therapy for stages I-III non-metastatic non-small-cell lung cancer. Nat Rev Clin Oncol 18: 547-557, 2021.
4. Li BT, Smit EF, Goto Y, Nakagawa K, Udagawa H, Mazières J, Nagasaka M, Bazhenova L, Saltos AN, Felip E, *et al*: Trastuzumab deruxtecan in HER2-mutant non-small-cell lung cancer. N Engl J Med 386: 241-251, 2022.
5. Sezer A, Kilickap S, Gümüş M, Bondarenko I, Özgüroğlu M, Gogishvili M, Turk HM, Cicin I, Bentsion D, Gladkov O, *et al*: Cemiplimab monotherapy for first-line treatment of advanced non-small-cell lung cancer with PD-L1 of at least 50%: A multicentre, open-label, global, phase 3, randomised, controlled trial. Lancet 397: 592-604, 2021.
6. Han J, Liu Y, Yang S, Wu X, Li H and Wang Q: MEK inhibitors for the treatment of non-small cell lung cancer. J Hematol Oncol 14: 1, 2021.
7. Paz-Ares L, Ciuleanu TE, Cobo M, Schenker M, Zurawski B, Menezes J, Richardet E, Bennouna J, Felip E, Juan-Vidal O, *et al*: First-line nivolumab plus ipilimumab combined with two cycles of chemotherapy in patients with non-small-cell lung cancer (CheckMate 9LA): An international, randomised, open-label, phase 3 trial. Lancet Oncol 22: 198-211, 2021.
8. Hanna NH, Robinson AG, Temin S, Baker S Jr, Brahmer JR, Ellis PM, Gaspar LE, Haddad RY, Hesketh PJ, Jain D, *et al*: Therapy for stage IV non-small-cell lung cancer with driver alterations: ASCO and OH (CCO) joint guideline update. J Clin Oncol 39: 1040-1091, 2021.
9. Niu Z, Jin R, Zhang Y and Li H: Signaling pathways and targeted therapies in lung squamous cell carcinoma: Mechanisms and clinical trials. Signal Transduct Target Ther 7: 353, 2022.
10. Li L, Li WJ, Zheng XR, Liu QL, Du Q, Lai YJ and Liu SQ: Eriodictyol ameliorates cognitive dysfunction in APP/PS1 mice by inhibiting ferroptosis via vitamin D receptor-mediated Nrf2 activation. Mol Med 28: 11, 2022.
11. Chen X, Kang R, Kroemer G and Tang D: Broadening horizons: The role of ferroptosis in cancer. Nat Rev Clin Oncol 18: 280-296, 2021.
12. Feng L, Zhao K, Sun L, Yin X, Zhang J, Liu C and Li B: SLC7A11 regulated by NRF2 modulates esophageal squamous cell carcinoma radiosensitivity by inhibiting ferroptosis. J Transl Med 19: 367, 2021.
13. Tang C, Yu M, Ma J and Zhu Y: Metabolic classification of bladder cancer based on multi-omics integrated analysis to predict patient prognosis and treatment response. J Transl Med 19: 205, 2021.
14. Chen X, Kang R, Kroemer G and Tang D: Targeting ferroptosis in pancreatic cancer: A double-edged sword. Trends Cancer 7: 891-901, 2021.
15. Tang R, Xu J, Zhang B, Liu J, Liang C, Hua J, Meng Q, Yu X and Shi S: Ferroptosis, necroptosis, and pyroptosis in anticancer immunity. J Hematol Oncol 13: 110, 2020.
16. Liu Z, Zhao Q, Zuo ZX, Yuan SQ, Yu K, Zhang Q, Zhang X, Sheng H, Ju HQ, Cheng H, *et al*: Systematic analysis of the aberrances and functional implications of ferroptosis in cancer. iScience 23: 101302, 2020.
17. Yang H, Yan M, Li W and Xu L: SIRPα and PD1 expression on tumor-associated macrophage predict prognosis of intrahepatic cholangiocarcinoma. J Transl Med 20: 140, 2022.
18. Cao W, Fan W, Wang F, Zhang Y, Wu G, Shi X, Shi JX, Gao F, Yan M, Guo R, *et al*: GM-CSF impairs erythropoiesis by disrupting erythroblastic island formation via macrophages. J Transl Med 20: 11, 2022.
19. Li W, Wang Y, Zhao H, Zhang H, Xu Y, Wang S, Guo X, Huang Y, Zhang S, Han Y, *et al*: Identification and transcriptome analysis of erythroblastic island macrophages. Blood 134: 480-491, 2019.
20. Wang Y, Li W, Schulz VP, Zhao H, Qu X, Qi Q, Cheng Y, Guo X, Zhang S, Wei X, *et al*: Impairment of human terminal erythroid differentiation by histone deacetylase 5 deficiency. Blood 138: 1615-1627, 2021.
21. Xu L, Yang H, Yan M and Li W: Matrix metalloproteinase 1 is a poor prognostic biomarker for patients with hepatocellular carcinoma. Clin Exp Med 23: 2065-2083, 2023.
22. Li W, Li T, Sun C, Du Y, Chen L, Du C, Shi J and Wang W: Identification and prognostic analysis of biomarkers to predict the progression of pancreatic cancer patients. Mol Med 28: 43, 2022.
23. Malta TM, Sokolov A, Gentles AJ, Burzykowski T, Poisson L, Weinstein JN, Kamińska B, Huelsken J, Omberg L, Gevaert O, *et al*: Machine learning identifies stemness features associated with oncogenic dedifferentiation. Cell 173: 338-354. e15, 2018.
24. Ralser DJ, Klümper N, Gevensleben H, Zarbl R, Kaiser C, Landsberg J, Hölzel M, Strieth S, Faridi A, Abramian A and Dietrich D: Molecular and immune correlates of PDCD1 (PD-1), PD-L1 (CD274), and PD-L2 (PDCD1LG2) DNA methylation in triple negative breast cancer. J Immunother 44: 319-324, 2021.
25. Wang M, Du Q, Jin J, Wei Y, Lu Y and Li Q: LAG3 and its emerging role in cancer immunotherapy. Clin Transl Med 11: e365, 2021.
26. Ascierto PA, Puzanov I, Agarwala SS, Blank C, Carvajal RD, Demaria S, Dummer R, Ernstoff M, Ferrone S, Fox BA, *et al*: Perspectives in melanoma: Meeting report from the 'melanoma bridge' (December 5th-7th, 2019, Naples, Italy). J Transl Med 18: 346, 2020.
27. Liu Z, Zhang Y, Shi C, Zhou X, Xu K, Jiao D, Sun Z and Han X: A novel immune classification reveals distinct immune escape mechanism and genomic alterations: Implications for immunotherapy in hepatocellular carcinoma. J Transl Med 19: 5, 2021.
28. Okła K, Rajtak A, Czerwonka A, Bobiński M, Wawruszak A, Tarkowski R, Bednarek W, Szumiło J and Kotarski J: Accumulation of blood-circulating PD-L1-expressing M-MDSCs and monocytes/macrophages in pretreatment ovarian cancer patients is associated with soluble PD-L1. J Transl Med 18: 220, 2020.
29. Zhao B, Xia Y, Yang F, Wang Y, Wang Y, Wang Y, Dai C, Wang Y and Ma W: Molecular landscape of IDH-mutant astrocytoma and oligodendroglioma grade 2 indicate tumor purity as an underlying genomic factor. Mol Med 28: 34, 2022.

30. Ravi R, Noonan KA, Pham V, Bedi R, Zhavoronkov A, Ozerov IV, Makarev E, V Artemov A, Wysocki PT, Mehra R, *et al*: Bifunctional immune checkpoint-targeted antibody-ligand traps that simultaneously disable TGFβ enhance the efficacy of cancer immunotherapy. Nat Commun 9: 741, 2018.
31. Zeng D, Li M, Zhou R, Zhang J, Sun H, Shi M, Bin J, Liao Y, Rao J and Liao W: Tumor microenvironment characterization in gastric cancer identifies prognostic and immunotherapeutically relevant gene signatures. Cancer Immunol Res 7: 737-750, 2019.
32. Wang J, Sun J, Liu LN, Flies DB, Nie X, Toki M, Zhang J, Song C, Zarr M, Zhou X, *et al*: Siglec-15 as an immune suppressor and potential target for normalization cancer immunotherapy. Nat Med 25: 656-666, 2019.
33. Jiang P, Gu S, Pan D, Fu J, Sahu A, Hu X, Li Z, Traugh N, Bu X, Li B, *et al*: Signatures of T cell dysfunction and exclusion predict cancer immunotherapy response. Nat Med 24: 1550-1558, 2018.
34. Wei J, Huang K, Chen Z, Hu M, Bai Y, Lin S and Du H: Characterization of glycolysis-associated molecules in the tumor microenvironment revealed by pan-cancer tissues and lung cancer single cell data. Cancers (Basel) 12: 1788, 2020.
35. Wood DE: National comprehensive cancer network (NCCN) Clinical practice guidelines for lung cancer screening. Thorac Surg Clin 25: 185-197, 2015.
36. Magaki S, Hojat SA, Wei B, So A and Yong WH: An introduction to the performance of immunohistochemistry. Methods Mol Biol 1897: 289-298, 2019.
37. Friedmann Angeli JP, Krysko DV and Conrad M: Ferroptosis at the crossroads of cancer-acquired drug resistance and immune evasion. Nat Rev Cancer 19: 405-414, 2019.
38. Wu Q, Qian W, Sun X and Jiang S: Small-molecule inhibitors, immune checkpoint inhibitors, and more: FDA-approved novel therapeutic drugs for solid tumors from 1991 to 2021. J Hematol Oncol 15: 143, 2022.
39. Passaro A, Brahmer J, Antonia S, Mok T and Peters S: Managing resistance to immune checkpoint inhibitors in lung cancer: Treatment and novel strategies. J Clin Oncol 40: 598-610, 2022.
40. Zhang D, Tang DG and Rycaj K: Cancer stem cells: Regulation programs, immunological properties and immunotherapy. Semin Cancer Biol 52: 94-106, 2018.
41. Clara JA, Monge C, Yang Y and Takebe N: Targeting signalling pathways and the immune microenvironment of cancer stem cells-a clinical update. Nat Rev Clin Oncol 17: 204-232, 2020.
42. Hänzelmann S, Castelo R and Guinney J: GSVA: Gene set variation analysis for microarray and RNA-seq data. BMC Bioinformatics 14: 7, 2013.
43. Cescon DW, She D, Sakashita S, Zhu CQ, Pintilie M, Shepherd FA and Tsao MS: NRF2 pathway activation and adjuvant chemotherapy benefit in lung squamous cell carcinoma. Clin Cancer Res 21: 2499-2505, 2015.
44. Ruiz EJ, Diefenbacher ME, Nelson JK, Sancho R, Pucci F, Chakraborty A, Moreno P, Annibaldi A, Liccardi G, Encheva V, *et al*: LUBAC determines chemotherapy resistance in squamous cell lung cancer. J Exp Med 216: 450-465, 2019.
45. Geeleher P, Cox NJ and Huang RS: Clinical drug response can be predicted using baseline gene expression levels and in vitro drug sensitivity in cell lines. Genome Biol 15: R47, 2014.
46. Goldstraw P, Chansky K, Crowley J, Rami-Porta R, Asamura H, Eberhardt WE, Nicholson AG, Groome P, Mitchell A, Bolejack V, *et al*: The IASLC lung cancer staging project: Proposals for revision of the TNM stage groupings in the forthcoming (eighth) edition of the TNM classification for lung cancer. J Thorac Oncol 11: 39-51, 2016.
47. Siegel RL, Miller KD, Fuchs HE and Jemal A: Cancer statistics, 2022. CA Cancer J Clin 72: 7-33, 2022.
48. Guo L, Ma Y, Ward R, Castranova V, Shi X and Qian Y: Constructing molecular classifiers for the accurate prognosis of lung adenocarcinoma. Clin Cancer Res 12: 3344-3354, 2006.
49. Selvaraj G, Kaliamurthi S, Kaushik AC, Khan A, Wei YK, Cho WC, Gu K and Wei DQ: Identification of target gene and prognostic evaluation for lung adenocarcinoma using gene expression meta-analysis, network analysis and neural network algorithms. J Biomed Inform 86: 120-134, 2018.
50. Shi X, Li R, Dong X, Chen AM, Liu X, Lu D, Feng S, Wang H and Cai K: IRGS: An immune-related gene classifier for lung adenocarcinoma prognosis. J Transl Med 18: 55, 2020.
51. Cui J, Wen Q, Tan X, Chen Z and Liu G: A genomic-clinicopathologic nomogram predicts survival for patients with laryngeal squamous cell carcinoma. Dis Markers 2019: 5980567, 2019.
52. Cui J, Wang L, Tan G, Chen W, He G, Huang H, Chen Z, Yang H, Chen J and Liu G: Development and validation of nomograms to accurately predict risk of recurrence for patients with laryngeal squamous cell carcinoma: Cohort study. Int J Surg 76: 163-170, 2020.
53. Chen P, Wu Q, Feng J, Yan L, Sun Y, Liu S, Xiang Y, Zhang M, Pan T, Chen X, *et al*: Erianin, a novel dibenzyl compound in Dendrobium extract, inhibits lung cancer cell growth and migration via calcium/calmodulin-dependent ferroptosis. Signal Transduct Target Ther 5: 51, 2020.
54. Fu X, Liu J, Liu D, Zhou Y, Guo Y, Wang Z, Yang S, He W, Chen P, Wang X, *et al*: Glucose-regulated protein 78 modulates cell growth, epithelial-mesenchymal transition, and oxidative stress in the hyperplastic prostate. Cell Death Dis 13: 78, 2022.
55. Xia S, Duan W, Liu W, Zhang X and Wang Q: GRP78 in lung cancer. J Transl Med 19: 118, 2021.
56. Wang W, Green M, Choi JE, Gijón M, Kennedy PD, Johnson JK, Liao P, Lang X, Kryczek I, Sell A, *et al*: $CD8^+$ T cells regulate tumour ferroptosis during cancer immunotherapy. Nature 569: 270-274, 2019.
57. Xu H, Ye D, Ren M, Zhang H and Bi F: Ferroptosis in the tumor microenvironment: Perspectives for immunotherapy. Trends Mol Med 27: 856-867, 2021.
58. Torres-Ayuso P, An E, Nyswaner KM, Bensen RC, Ritt DA, Specht SI, Das S, Andresson T, Cachau RE, Liang RJ, *et al*: TNIK Is a therapeutic target in lung squamous cell carcinoma and regulates FAK activation through merlin. Cancer Discov 11: 1411-1423, 2021.